

Analysis of optical waveguides with arbitrary index profile using an immersed interface method

Theodoros P. Horikis

Department of Mathematics, University of Ioannina, Ioannina 45110, Greece

Abstract

A numerical technique is described that can efficiently compute solutions in interface problems. These are problems with data, such as the coefficients of differential equations, discontinuous or even singular across one or more interfaces. A prime example of these problems are optical waveguides and as such the scheme is applied to Maxwell's equations as they are formulated to describe light confinement in Bragg fibers. It is based on standard finite differences appropriately modified to take into account all possible discontinuities across the waveguide's interfaces due to the change of the refractive index. Second and fourth order schemes are described with additional adaptations to handle matrix eigenvalue problems, demanding geometries and defects.

Keywords: Finite differences, immersed interface method, high order finite difference method, coordinate stretching, Bragg fibers

PACS: 02.70.Bf, 02.60.Lj, 02.60.Cb, 42.81.Qb, 41.20.Jb

Light confinement due to cylindrical Bragg reflection instead of total internal reflection was first proposed more than three decades ago [1] and gave birth to the so-called Bragg fibers. These fibers attract considerable interest because of their ability to guide light in an air core; they are essentially dielectric coaxial fibers comprised of alternating circular layers with different indices of refraction. The key to making these fibers confine light efficiently, i.e., have low absorption loss and a high threshold power for nonlinear effects, is to use materials with a high index contrast [2, 3, 4, 5]. However, the high index contrast and the layered structure that gives these fibers their unique properties also makes them difficult to model.

Mathematically, these problems are called interface problems since their input data (such as the coefficients of differential equations, source terms etc.) may be discontinuous or even singular across one or several interfaces. The solution to an interface problem, therefore, typically is non-smooth or even discontinuous across the interfaces. Interface problems occur in many physical applications, particularly for free boundary/moving interface problems, such as, the modeling of the Stefan problem of solidification process and crystal growth, composite materials, multi-phase flows, cell and bubble deformation, and many others [14].

Several methods have been proposed to study these problems, including asymptotic analysis [6], the transfer matrix method [7], finite element methods [8, 9], special func-

tions –Bessel [10] and Hankel [11]– formalism, and Galerkin numerical methods [12, 13]. A comparative analysis of the most commonly used methods has also been published [7], demonstrating the capabilities and limitations of each method. Among the different numerical solution methods, the finite difference (FD) method is more attractive due to its advantage of simple formulation and numerical implementation and thus will be used here to analyze these problem.

Our approach is based on the immersed interface method [15] (IIM) which has been attracting considerable attention due to the many physical problems that can be applied on [16, 17, 18, 19, 20, 21, 22, 23, 24]. This approach has two additional advantages over standard Galerkin methods [12]. First of all, the scheme does not need to be modified significantly if different boundary conditions are used, thus allowing to calculate all possible solutions without any modifications. Methods based upon the Galerkin method typically require a set of basis functions that naturally satisfy the boundary conditions, hence the solution must be reformulated in a significant way if these change. More importantly, the IIM does not depend on any specific functional representation of solutions. Hence, cumbersome integrations or finding roots of nontrivial functions, such as Bessel functions (even when asymptotically approximated [6]), are avoided.

The essence of the method is to appropriately modify the correct matrix elements of a standard (central) FD scheme so as to take into account all discontinuities across interfaces. Starting with a differential equation and under a FD approximation one transforms the equation into an algebraic system of the form

$$A\mathbf{x} = \mathbf{b}$$

where \mathbf{x} is the solution or

$$A\mathbf{x} = \lambda\mathbf{x}$$

for eigenvalue problems, where λ is the eigenvalue. The matrix A is comprised of zero elements except for the main, upper and lower diagonal (for second order accurate solutions or more for more accurate schemes), i.e.

$$A = \begin{pmatrix} a_{11} & a_{12} & 0 & \cdots & 0 \\ a_{21} & a_{22} & a_{23} & \cdots & 0 \\ 0 & a_{32} & a_{33} & a_{34} & \cdots \\ 0 & 0 & \ddots & \ddots & \ddots \end{pmatrix}$$

This feature gives the FD method an additional advantage since A is tridiagonal. Using sparse matrix algebra one can significantly lower computational time, whether the inverse of the matrix or the eigenvalues is sought for. The goal is to identify the elements where the interface occurs and correct the appropriate matrix elements in a way described below to take into account the effects of the interfaces. Remarkably, these corrections are solutions of linear algebraic systems of equations. Thus, the matrix remains sparse and computational time is kept to a minimum.

The original formulation [15] of the IIM does not consider eigenvalue problems such as the problems of interest here. Hence, in order to deal with waveguide problems for Bragg fibers,

the method must be extended to handle any eigenvalue problem described by a second order differential operator. Moreover, the method must be extended to handle coupled equations like the ones describing the two polarization components of the electromagnetic field. Furthermore, since the method is based on finite differences one can use higher order schemes to increase the accuracy of the calculations. The extension to higher order accuracy is also presented in this article. However, extending to higher order posses a major limitation. In some problems, the geometry of the interfaces are such that in order to have enough points between them (using a uniform grid) requires to increase the total number of points and as such computational time. To overcome this, we introduce a coordinate stretching transformation which allows the method to handle these more demanding geometries.

The article is organized as follows: We begin with the description of the method in second order. In so doing, we extend the original formulation of the IIM to matrix eigenvalue problems. In addition, it is shown that all discontinuities/singularities are removed from the equation and passed on the FD scheme as corrections to the standard FD coefficients based on matching conditions across an interface. These corrections are calculated using linear systems of algebraic equations. Then fibers with deformations are considered to further illustrate the versatility of the method. Finally, we extend to fourth order and conclude with more demanding geometries in which the original IIM would fail unless a coordinate stretching is applied.

1. Formulation

The vector Helmholtz equations in cylindrical coordinates for the magnetic field are [25]

$$\nabla_t^2 H_r - \frac{2}{r^2} \frac{\partial H_\theta}{\partial \theta} - \frac{1}{r^2} H_r + k^2 n^2 H_r = \beta^2 H_r \quad (1a)$$

$$\nabla_t^2 H_\theta - \frac{1}{r} \frac{d(\ln n^2)}{dr} \frac{\partial}{\partial r} (r H_\theta) + \frac{1}{r} \left[\frac{d(\ln n^2)}{dr} + \frac{2}{r} \right] \frac{\partial H_r}{\partial \theta} - \frac{1}{r^2} H_\theta + k^2 n^2 H_\theta = \beta^2 H_\theta \quad (1b)$$

$$H_z = \frac{i}{\beta} \frac{1}{r} \left[\frac{\partial}{\partial r} (r H_r) + \frac{\partial H_\theta}{\partial \theta} \right] \quad (1c)$$

where k is the wavenumber, $n = n(r)$ is the (arbitrary) index of refraction, and β is the propagation constant. We focus on the first two equations, since the components of the electrical field, E_r , E_θ and E_z , as well as the transverse magnetic field, H_z can be recovered from H_r and H_θ using Maxwell's equations. All fields of the guiding modes are assumed to go to zero as $r \rightarrow \infty$. In addition, in order for system (1) to be well defined at the origin, the following boundary conditions must hold at $r = 0$

$$\frac{\partial^2 H_\theta}{\partial \theta^2} - H_\theta + 2 \frac{\partial H_r}{\partial \theta} = 0 \quad (2a)$$

$$\frac{\partial^2 H_r}{\partial \theta^2} - H_r - 2 \frac{\partial H_\theta}{\partial \theta} = 0 \quad (2b)$$

Separation of variables in Eqs. (1) suggests that the fields can be expressed in the form $H_r(r, \theta) = H_{rm}(r) \cos(m\theta)$ and $H_\theta(r, \theta) = H_{\theta m}(r) \sin(m\theta)$ with m an integer. Hence,

Eqs. (1) become

$$\frac{1}{r} \frac{d}{dr} \left(r \frac{dH_{rm}}{dr} \right) - \frac{1}{r^2} [(1 + m^2)H_{rm} + 2mH_{\theta m}] + k^2 n^2 H_{rm} = \beta^2 H_{rm} \quad (3a)$$

$$\begin{aligned} \frac{n^2}{r} \frac{d}{dr} \left[\frac{1}{n^2} \left(r \frac{dH_{\theta m}}{dr} + H_{\theta m} + mH_{rm} \right) \right] - \frac{1}{r^2} [2mH_{rm} + (1 + m^2)H_{\theta m}] \\ - \frac{1}{r} \frac{d}{dr} (mH_{rm} + H_{\theta m}) + k^2 n^2 H_{\theta m} = \beta^2 H_{\theta m} \end{aligned} \quad (3b)$$

In the absence of angular dependence, i.e., $m = 0$, these equations uncouple and describe the TE and TM modes of the fiber, respectively. Hereafter we drop the double subscript notation and we set $H_{rm} = H_r(r)$ and $H_{\theta m} = H_\theta(r)$. The boundary conditions as $r \rightarrow \infty$ remain the same and at $r = 0$ Eqs. (2) become

$$(1 + m^2)H_r + 2mH_\theta = 0 \quad (4a)$$

$$2mH_r + (1 + m^2)H_\theta = 0 \quad (4b)$$

When $m \neq 1$ these simply imply that $H_r(r = 0) = H_\theta(r = 0) = 0$. When $m = 1$, however, Eqs. (4) are identical and an additional boundary condition must be imposed. It is straightforward to show via a Taylor series expansion around $r = 0$ that the solution will satisfy the condition

$$\frac{d}{dr}(H_r - H_\theta) = 0$$

which we will impose as our additional boundary condition. The way to implement these boundary conditions into the FD scheme is shown in the appendix.

2. The second order method

Consider the system of coupled equations that describe the electric, H_r , and magnetic, H_θ , fields in a circular waveguide, Eqs. (3). Expanding all derivatives in Eqs. (3) and after appropriate simplifications the system is written as

$$\frac{d^2 H_r}{dr^2} + \frac{1}{r} \frac{dH_r}{dr} - \frac{2m}{r^2} H_\theta + \left(k^2 n^2 - \frac{m^2 + 1}{r^2} \right) H_r = \beta^2 H_r \quad (5a)$$

$$\frac{d^2 H_\theta}{dr^2} + \left(-\frac{2n'}{n} + \frac{1}{r} \right) \frac{dH_\theta}{dr} - m \left(\frac{2n'}{nr} + \frac{2}{r^2} \right) H_r + \left(k^2 n^2 - \frac{m^2 + 1}{r^2} - \frac{2n'}{nr} \right) H_\theta = \beta^2 H_\theta \quad (5b)$$

and the prime ('') denotes differentiation with respect to r . Consider a finite difference approximation for Eqs. (5) of the form (central differences)

$$\gamma_1 H_{r,i-1} + \gamma_2 H_{r,i} + \gamma_3 H_{r,i+1} + \Delta H_{\theta,i} = \beta^2 H_{r,i} \quad (6a)$$

$$\delta_1 H_{\theta,i-1} + \delta_2 H_{\theta,i} + \delta_3 H_{\theta,i+1} + \Gamma H_{r,i} = \beta^2 H_{\theta,i} \quad (6b)$$

where (see appendix)

$$\gamma_1 = \delta_1 = \frac{1}{h^2} - \frac{1}{2hr_i}, \quad \gamma_2 = \delta_2 = -\frac{2}{h^2} + k^2 n^2 - \frac{1}{r_i^2}, \quad \gamma_3 = \delta_3 = \frac{1}{h^2} + \frac{1}{2hr_i}, \quad \Gamma = \Delta = -\frac{2m}{r_i^2}$$

with $r \in [a, b]$ defined on a uniform grid as

$$r_i = a + ih = a + i \left(\frac{b-a}{N} \right), \quad i = 0, 1, 2, \dots, N.$$

Using this one can find the correct row where the correction must be applied. If the interface occurs at $r = r^*$ then setting

$$r_i = r^* \Rightarrow j = \text{int} \left\{ \frac{r^* - a}{h} \right\}$$

gives the row to be corrected. The function $\text{int}\{\cdot\}$ denotes integer part.

In Eq. (5) the index of refraction is a discontinuous function and changes, say, at $r = r^*$, so that

$$n(r) = \begin{cases} n_1, & r < r^* \\ n_2, & r > r^* \end{cases}$$

The above scheme cannot be used without any modifications as it does not take into consideration the singularities appearing in the equations due to the form of the index of refraction. Thus we reformulate the problem, including the differential equations, in vector form. In addition, the terms including derivatives of discontinuous functions are neglected (we assume the index is piecewise constant) and their contribution is incorporated into the finite difference scheme through appropriate jump conditions on the interfaces. In so doing, Eqs. (5) read in vector form

$$\mathbf{H}_{rr} + \frac{1}{r} \mathbf{H}_r + B \mathbf{H} = \beta^2 \mathbf{H} \quad (7)$$

where $\mathbf{H} = (H_r, H_\theta)^T$ and

$$B = \begin{pmatrix} k^2 n^2 - (m^2 + 1)/r^2 & -2m/r^2 \\ -2m/r^2 & k^2 n^2 - (m^2 + 1)/r^2 \end{pmatrix}$$

In the vector formulation subscripts denote differentiation.

The goal is to determine the coefficients of the finite difference approximation (6) to take into account this jump of the refractive index at $r = r^*$. To do this, divide the region $[a, b]$ into two, the $(-)$ region for $r < r^*$ and the $(+)$ region for $r > r^*$, as in Fig. 1. The analysis is similar for the two regions, but needs to be repeated for both. Start with the $(-)$ region: we need to replace \mathbf{H}_{i-1} , \mathbf{H}_i , \mathbf{H}_{i+1} in Eqs. (6) so that the local truncation error is first order. Expand \mathbf{H} around the points before and after the jump, namely

$$\mathbf{H}(r_{j-1}) = \mathbf{H}_{j-1} = \mathbf{H}^- + (r_{j-1} - r^*) \mathbf{H}_r^- + \frac{1}{2} (r_{j-1} - r^*)^2 \mathbf{H}_{rr}^- \quad (8a)$$

$$\mathbf{H}(r_j) = \mathbf{H}_j = \mathbf{H}^- + (r_j - r^*) \mathbf{H}_r^- + \frac{1}{2} (r_j - r^*)^2 \mathbf{H}_{rr}^- \quad (8b)$$

$$\mathbf{H}(r_{j+1}) = \mathbf{H}_{j+1} = \mathbf{H}^+ + (r_{j+1} - r^*) \mathbf{H}_r^+ + \frac{1}{2} (r_{j+1} - r^*)^2 \mathbf{H}_{rr}^+ \quad (8c)$$

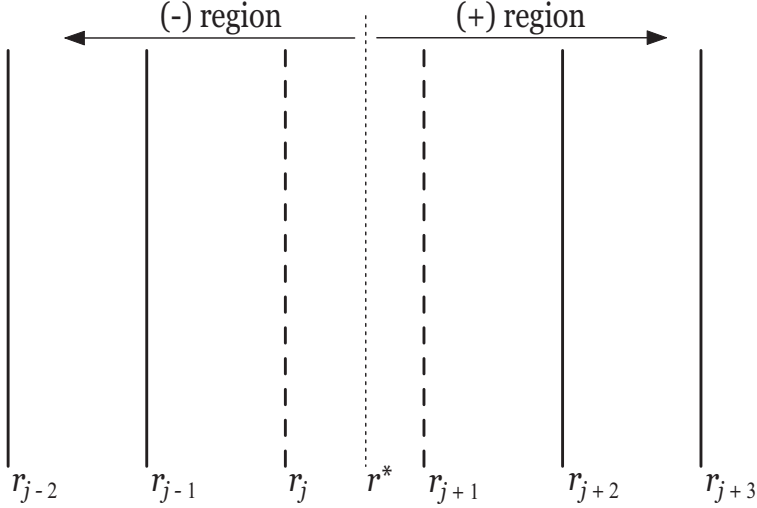


Figure 1: The $(-)$ and $(+)$ regions, the problematic point $r = r^*$ and the irregular grid points r_j and r_{j+1} .

The index j denotes points closest to the jump, as in Fig. 1. Notice that we only include second order terms in the expansions. We need to replace the $(+)$ functions in Eq. (8c) since we are in the $(-)$ region; this is done through the continuity conditions.

To derive these continuity or matching conditions one needs to refer to the physical properties of the problem. Here all fields are continuous functions across all interfaces, i.e.

$$\begin{aligned} H_r^+ &= H_r^- \\ H_\theta^+ &= H_\theta^- \\ H_z^+ &= H_z^- \end{aligned}$$

The last equation and Eq. (1c) also yield (recall that all fields are only functions of r)

$$\frac{i}{\beta} \frac{1}{r^*} \left(H_r^+ r^* \frac{d}{dr} H_r^+ \right) = \frac{i}{\beta} \frac{1}{r^*} \left(H_r^- r^* \frac{d}{dr} H_r^- \right)$$

or

$$\frac{d}{dr} H_r^+ = \frac{d}{dr} H_r^-$$

Another condition may be derived by integrating Eq. (3b) around $r = r^*$, namely

$$\begin{aligned} \lim_{\Delta r \rightarrow 0} \int_{r^* - \Delta r}^{r^* + \Delta r} \left\{ \frac{n^2}{r} \frac{d}{dr} \left[\frac{1}{n^2} \left(r \frac{dH_\theta}{dr} + H_\theta + mH_r \right) \right] - \frac{1}{r^2} [2mH_r + (1 + m^2)H_\theta] \right\} \\ - \lim_{\Delta r \rightarrow 0} \int_{r^* - \Delta r}^{r^* + \Delta r} \left\{ \frac{1}{r} \frac{d}{dr} (mH_r + H_\theta) + k^2 n^2 H_\theta \right\} = \lim_{\Delta r \rightarrow 0} \int_{r^* - \Delta r}^{r^* + \Delta r} \{\beta^2 H_\theta\} \end{aligned}$$

and since all fields are continuous across $r = r^*$ the only nonzero remaining terms are

$$\begin{aligned} \frac{1}{n_2^2} \left(r^* \frac{dH_\theta^+}{dr} + H_\theta^+ + mH_r^+ \right) - (mH_r^+ + H_\theta^+) &= \\ \frac{1}{n_1^2} \left(r^* \frac{dH_\theta^-}{dr} + H_\theta^- + mH_r^- \right) - (mH_r^- + H_\theta^-) & \end{aligned}$$

Finally, the matching conditions for the second derivatives are a consequence of the continuity of the fields and Eqs. (5) since

$$\mathbf{H}^- = \mathbf{H}^+ \Leftrightarrow \beta^2 \mathbf{H}^- = \beta^2 \mathbf{H}^+$$

which results in

$$\mathbf{H}_{rr}^+ + \frac{1}{r^*} \mathbf{H}_r^+ + B^+ \mathbf{H}^+ = \mathbf{H}_{rr}^- + \frac{1}{r^*} \mathbf{H}_r^- + B^- \mathbf{H}^-$$

In summary, the continuity conditions in vector form are

$$\mathbf{H}^- = \mathbf{H}^+ \tag{9a}$$

$$\mathbf{H}_r^+ = C\mathbf{H}_r^- + D\mathbf{H} \tag{9b}$$

$$\mathbf{H}_{rr}^+ = \mathbf{H}_{rr}^- + E\mathbf{H}_r^- + F\mathbf{H} \tag{9c}$$

where

$$\begin{aligned} C &= \begin{pmatrix} 1 & 0 \\ 0 & n_2^2/n_1^2 \end{pmatrix}, \quad D = \frac{n_2^2/n_1^2 - 1}{r^*} \begin{pmatrix} 0 & 0 \\ m & 1 \end{pmatrix}, \quad E = -\frac{n_2^2/n_1^2 - 1}{r^*} \begin{pmatrix} 0 & 0 \\ 0 & 1 \end{pmatrix}, \\ F &= - \begin{pmatrix} k(n_2^2 - n_1^2) & 0 \\ m(n_2^2/n_1^2 - 1)/r^{*2} & (n_2^2/n_1^2 - 1)/r^{*2} + k(n_2^2 - n_1^2) \end{pmatrix} \end{aligned}$$

To put everything together return to the FD approximation in matrix form

$$\Gamma_1 \mathbf{H}_{i-1} + \Gamma_2 \mathbf{H}_i + \Gamma_3 \mathbf{H}_{i+1} = \beta^2 \mathbf{H}_i$$

where the scalar coefficients γ 's are replaced by 2×2 matrices. Replacing \mathbf{H}_{j-1} , \mathbf{H}_j and \mathbf{H}_{j+1} from Eqs. (8), using Eqs. (9) and

$$\beta^2 \mathbf{H}_j = \mathbf{H}_{rr}^- + \frac{1}{r^*} \mathbf{H}_r^- + B^- \mathbf{H}$$

we obtain an equality with \mathbf{H}_{rr}^- , \mathbf{H}_r^- and \mathbf{H} on both sides. Matching the relative coefficients results in the following linear system for the coefficients at $r_j \leq r^*$

$$\begin{aligned} \Gamma_1 + \Gamma_2 + \Gamma_3 \left[I_2 + (r_{j+1} - r^*)D + \frac{1}{2}(r_{j+1} - r^*)^2 F \right] &= B^- \\ (r_{j-1} - r^*)\Gamma_1 + (r_j - r^*)\Gamma_2 + \Gamma_3 \left[(r_{j+1} - r^*)C + \frac{1}{2}(r_{j+1} - r^*)^2 E \right] &= \frac{1}{r^*} I_2 \\ \frac{1}{2}(r_{j-1} - r^*)^2 \Gamma_1 + \frac{1}{2}(r_j - r^*)^2 \Gamma_2 + \frac{1}{2}(r_{j+1} - r^*)^2 \Gamma_3 &= I_2 \end{aligned}$$

and at $r_{j+1} > r^*$

$$\begin{aligned}\Gamma_1 \left[I_2 - (r_j - r^*) C^{-1} D + \frac{1}{2} (r_j - r^*)^2 F_2 \right] + \Gamma_2 + \Gamma_3 &= B^+ \\ \Gamma_1 \left[(r_j - r^*) C^{-1} + \frac{1}{2} (r_j - r^*)^2 E_2 \right] + (r_{j+1} - r^*) \Gamma_2 + \Gamma_3 (r_{j+2} - r^*) &= \frac{1}{r^*} I_2 \\ \frac{1}{2} (r_j - r^*)^2 \Gamma_1 + \frac{1}{2} (r_{j+1} - r^*)^2 \Gamma_2 + \frac{1}{2} (r_{j+2} - r^*)^2 \Gamma_3 &= I_2\end{aligned}$$

where we need to introduce the matrices

$$\begin{aligned}E_2 &= \begin{pmatrix} 0 & 0 \\ 0 & (1 - n_1^2/n_2^2)/r^* \end{pmatrix}, \\ F_2 &= \begin{pmatrix} k^2(n_2^2 - n_1^2) & 0 \\ m(1 - n_1^2/n_2^2)/r^* & k^2(n_2^2 - n_1^2) - (1 - n_1^2/n_2^2)/r^{*2} \end{pmatrix}\end{aligned}$$

For the latter system (the (+) side, $r_{j+1} > r^*$) Eqs. (9) were inverted to substitute for the (-) side. Each of the above systems represents a 12×12 system of algebraic equations that determines the coefficients of the matrices. If multiple interfaces are present, one merely applies these difference formulas multiple times. Note that the result is a system of finite difference equations each involving three neighboring points making the resulting equations tridiagonal. Because of the tridiagonal structure of the matrix, sparse matrix algebra can be used to determine the eigenvalues and eigenmodes. Thus, a large number of points can be used for modest computational cost, which allows the accuracy of the results to be increased and the modes of complicated structures to be determined, e.g., Bragg fibers with many thin layers [5]. Also note that the corrections depend only on the values of the refractive index before and after the discontinuity. This means that the jump conditions do not have to be modified if the index varies radially between the discontinuities.

To test our method we use a Bragg fiber with an air core of radius $1.0 \mu\text{m}$ and a cladding that consists of alternating layers with refractive indices $n_1 = 3.0$ and $n_2 = 1.5$ [6, 12]. The distance between layers is $0.130 \mu\text{m}$ and $0.265 \mu\text{m}$. As done previously [12], an imaginary cladding with a refractive index close to zero is added outside the core to prevent reflections. For multilayer Bragg fibers the effective index, β/k , is usually measured instead of just β . Within the spectral range of $1.4 \mu\text{m} < \lambda < 1.6 \mu\text{m}$, the Bragg fiber supports a single TE mode, whose propagation constant effective index is plotted in Fig. 2.

This method can also be applied to more complicated and computationally demanding fibers. For example, let's consider the Omniduide fiber described in Ref. [5]. This is a large air-core fiber with core radius $13.02 \mu\text{m}$ surrounded by 17 layers, starting with a high-index layer, with indices $n_1 = 4.6$ and $n_2 = 1.6$, and thicknesses $l_1 = 0.09548 \mu\text{m}$ and $l_2 = 0.33852 \mu\text{m}$, respectively. Under these parameters the wavelength for the lowest dissipation losses is $\lambda = 1.55 \mu\text{m}$. The first two modes of the fiber, namely the TE_{01} and TE_{11} are plotted in Fig. 3. The effective indices are 0.99736632 and 1.00097643, respectively. The way to implement the additional boundary condition for the TE_{11} mode ($m = 1$) is described in the appendix.

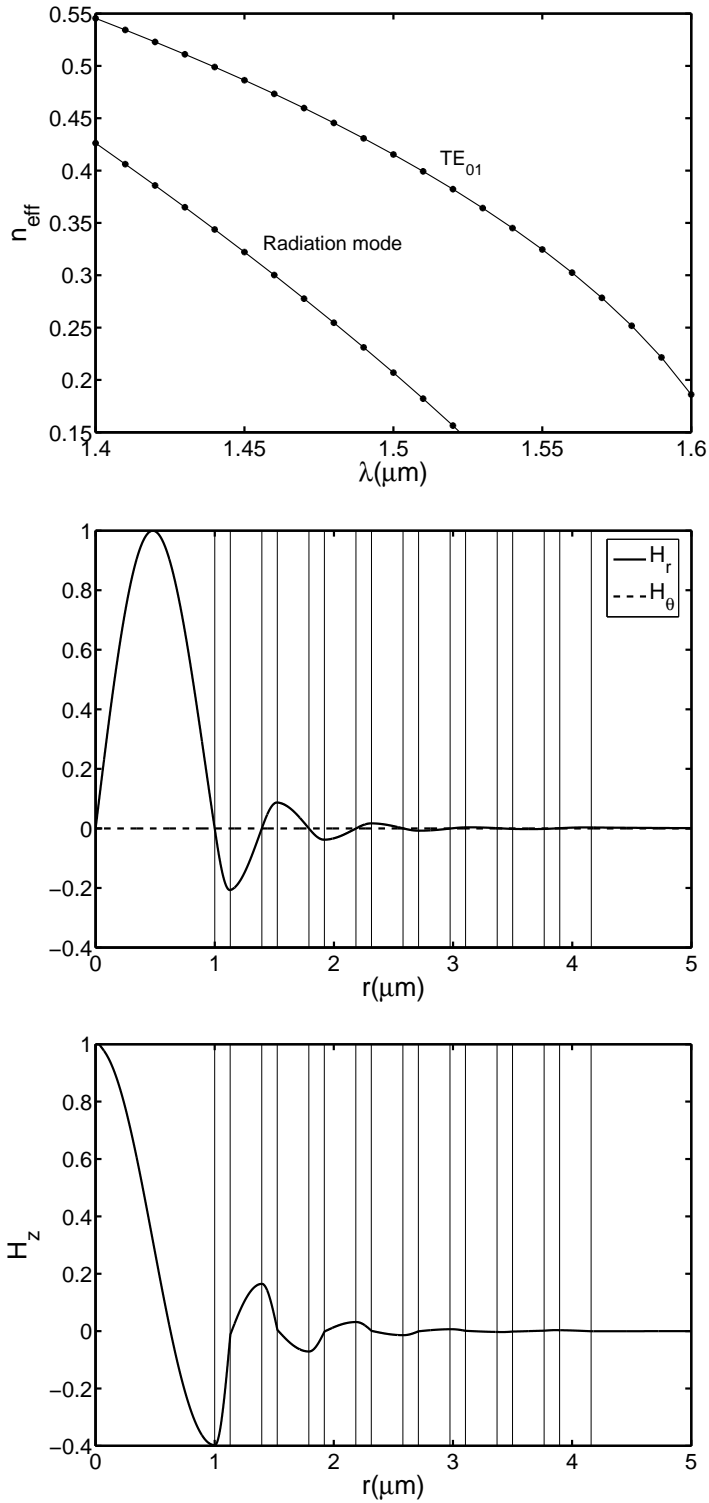


Figure 2: Dispersion (top) of the fundamental TE mode in the air-core Bragg fiber described in the text and in Refs. [6, 12] and the TE, TM (middle) and H_z (bottom) modes plotted at $\lambda = 1.55 \mu\text{m}$.

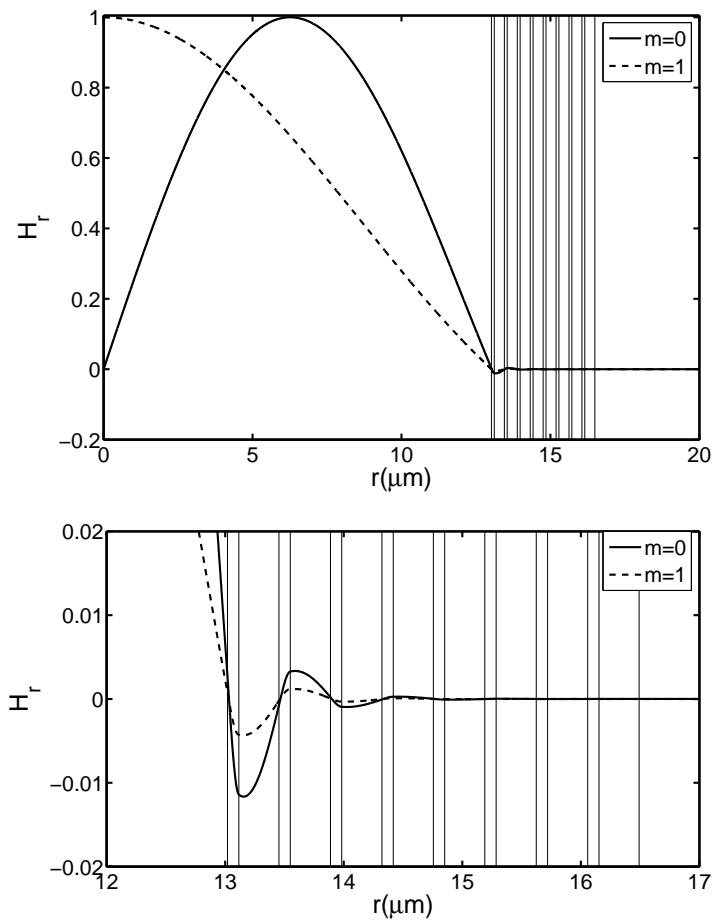


Figure 3: The fundamental TE mode and the TE_{11} mode of the air-core Omniduide fiber described in the text and in Ref. [5]. The bottom figure is a blow-up of the fields near the end of the fiber's core.

Notably, plastic optical fibers (POFs) which attracted recent attention because of their use in subscriber line systems and home networks also have a large core diameter and a high core-cladding refractive-index difference compared with conventional silica glass multimode optical fibers and can support tens of thousands to hundreds of thousands of propagation modes. A recent finite element method was used [8, 9] to analyze their properties. We discuss these (and more demanding geometries) at a later section.

3. Fibers with deformations

Single defects surrounded by Bragg reflectors as the basis for annular resonators were proposed and analyzed in Ref. [26]. The basic geometry was a circumferentially-guiding defect is located within a medium which consists of annular Bragg layers. As a result of the circular geometry, the layer widths, unlike in rectangular geometry, are not constant, and the task is to determine the widths that lead to maximum confinement in the defect. In addition, it has been suggested [27] that fibers with such defects can be used to model pairs of identical touching hollow Bragg fibers. The dielectric profile along the interfiber center line resembles a one-dimensional Bragg grating with a central defect formed by the two external layers of the fiber mirrors.

Figure 4 depicts the magnetic field inside a defect. The high index layers and the defect have an effective refractive index $n_1 = 2$ while the low index layers have an effective refractive index $n_2 = 1$. The internal and external Bragg reflectors have 10 periods, and the wavelength is $1.45\mu\text{m}$. The defect is $(\lambda/2)\mu\text{m}$ wide. The effective index is found to be 0.92257830.

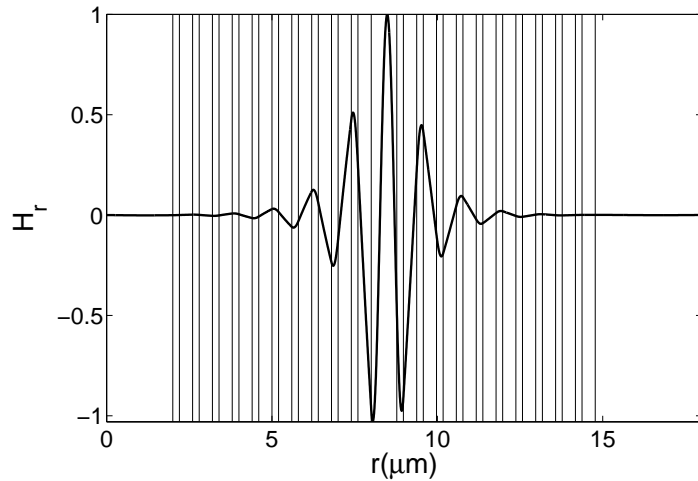


Figure 4: The magnetic field distribution of an annular defect mode resonator.

Resonant features correspond to the points of accidental degeneracy of TE_{01} with higher-order modes. This is true for this case and the effective indices for the TE_{01} and TE_{20} modes were found to be 0.87238117 and 0.49188825, respectively. For more details on the physical properties of these defects we refer the reader to [27].

4. Higher order method

Higher order accuracy methods can also be derived in a similar manner. The main focus is again Eqs. (3). As before, assume the refractive index to be piece-wise constant, and write these equations in vector form as

$$\mathbf{H}_{rr} + \frac{1}{r}\mathbf{H}_r + B_1\mathbf{H} = \beta^2\mathbf{H} \quad (10)$$

where $\mathbf{H} = (H_r, H_\theta)^T$,

$$B_1 = \begin{pmatrix} k^2 n^2 - (m^2 + 1)/r^2 & -2m/r^2 \\ -2m/r^2 & k^2 n^2 - (m^2 + 1)/r^2 \end{pmatrix}$$

and the subscripts denote differentiation. Recall, the continuity conditions are

$$\mathbf{H}^- = \mathbf{H}^+ \quad (11a)$$

$$\mathbf{H}_r^+ = C_1\mathbf{H}_r^- + D_1\mathbf{H} \quad (11b)$$

$$\mathbf{H}_{rr}^+ = \mathbf{H}_{rr}^- + E_1\mathbf{H}_r^- + F_1\mathbf{H} \quad (11c)$$

where

$$C_1 = \begin{pmatrix} 1 & 0 \\ 0 & n_2^2/n_1^2 \end{pmatrix}, \quad D_1 = \frac{n_2^2/n_1^2 - 1}{r^*} \begin{pmatrix} 0 & 0 \\ m & 1 \end{pmatrix}, \quad E_1 = -\frac{n_2^2/n_1^2 - 1}{r^*} \begin{pmatrix} 0 & 0 \\ 0 & 1 \end{pmatrix},$$

$$F_1 = - \begin{pmatrix} k(n_2^2 - n_1^2) & 0 \\ m(n_2^2/n_1^2 - 1)/r^{*2} & (n_2^2/n_1^2 - 1)/r^{*2} + k(n_2^2 - n_1^2) \end{pmatrix}$$

The fourth order finite difference approximation in matrix form is

$$\Gamma_1\mathbf{H}_{i-2} + \Gamma_2\mathbf{H}_{i-1} + \Gamma_3\mathbf{H}_i + \Gamma_4\mathbf{H}_{i+1} + \Gamma_5\mathbf{H}_{i+2} = \beta^2\mathbf{H}_i \quad (12)$$

where (see appendix)

$$\begin{aligned} \Gamma_1 &= \begin{pmatrix} -1/12h^2 + 1/12r_i h & 0 \\ 0 & -1/12h^2 + 1/12r_i h \end{pmatrix}, \\ \Gamma_2 &= \begin{pmatrix} 4/3h^2 - 2/3r_i h & 0 \\ 0 & 4/3h^2 - 2/3r_i h \end{pmatrix}, \\ \Gamma_3 &= \begin{pmatrix} k^2 n^2 - (m^2 + 1)/r_i^2 - 5/2h^2 & -2m/r_i^2 \\ -2m/r_i^2 & k^2 n^2 - (m^2 + 1)/r_i^2 - 5/2h^2 \end{pmatrix}, \\ \Gamma_4 &= \begin{pmatrix} 4/3h^2 + 2/3r_i h & 0 \\ 0 & 4/3h^2 + 2/3r_i h \end{pmatrix}, \\ \Gamma_5 &= \begin{pmatrix} 1/12h^2 - 1/12r_i h & 0 \\ 0 & -1/12h^2 - 1/12r_i h \end{pmatrix} \end{aligned}$$

at all regular points. We need to define these matrices for the irregular points using the IIM. We define our grid as before, namely $r_i = a + i\frac{b-a}{N}$, with N the total number of points,

and assume that the point $r = r^*$ is between two points, say r_j and r_{j+1} . As in the case of second order accuracy, we define a point to be regular if all points of the finite difference equation, Eq. (12), are on the same region, either the $(-)$ or the $(+)$ regions. All other points are irregular. Thus, in Fig. 1 the irregular points are r_{j-1}, r_j, r_{j+1} and r_{j+2} . We only need to define the Γ 's in Eq. (12) at these points.

To do so we need to expand in Taylor series all function around the problematic point $r = r^*$ up to and including terms of fourth order. Hence, for example at $r = r_j < r^*$

$$\begin{aligned}\mathbf{H}_{j-1} &= \mathbf{H} + (r_{j-1} - r^*)\mathbf{H}_r^- + \frac{1}{2}(r_{j-1} - r^*)^2\mathbf{H}_{rr}^- + \frac{1}{6}(r_{j-1} - r^*)^3\mathbf{H}_{rrr}^- + \frac{1}{24}(r_{j-1} - r^*)^4\mathbf{H}_{rrrr}^- \\ \mathbf{H}_j &= \mathbf{H} + (r_j - r^*)\mathbf{H}_r^- + \frac{1}{2}(r_j - r^*)^2\mathbf{H}_{rr}^- + \frac{1}{6}(r_j - r^*)^3\mathbf{H}_{rrr}^- + \frac{1}{24}(r_j - r^*)^4\mathbf{H}_{rrrr}^- \\ \mathbf{H}_{j+1} &= \mathbf{H} + (r_{j+1} - r^*)\mathbf{H}_r^+ + \frac{1}{2}(r_{j+1} - r^*)^2\mathbf{H}_{rr}^+ + \frac{1}{6}(r_{j+1} - r^*)^3\mathbf{H}_{rrr}^+ + \frac{1}{24}(r_{j+1} - r^*)^4\mathbf{H}_{rrrr}^+ \\ \mathbf{H}_{j+2} &= \mathbf{H} + (r_{j+2} - r^*)\mathbf{H}_r^+ + \frac{1}{2}(r_{j+2} - r^*)^2\mathbf{H}_{rr}^+ + \frac{1}{6}(r_{j+2} - r^*)^3\mathbf{H}_{rrr}^+ + \frac{1}{24}(r_{j+2} - r^*)^4\mathbf{H}_{rrrr}^+\end{aligned}$$

While the continuity conditions are known up to the second derivative, see Eqs. (11), additional are needed for the higher derivatives. These are obtained from differentiating Eq. (7) and using Eqs. (11). Hence for the third derivative

$$\mathbf{H}_{rrr}^+ + \frac{1}{r^*}\mathbf{H}_{rr}^+ + B_r\mathbf{H}_r^+ = \beta^2\mathbf{H}_r^+ = \beta^2(C_1\mathbf{H}_r^- + D_1\mathbf{H})$$

which after further use of Eqs. (7) and (11) becomes

$$\mathbf{H}_{rrr}^+ = C_3\mathbf{H}_{rrr}^- + D_3\mathbf{H}_{rr}^- + E_3\mathbf{H}_r^- + F_3\mathbf{H}$$

and similarly for the fourth derivative

$$\mathbf{H}_{rrrr}^+ = \mathbf{H}_{rrrr}^- + C_5\mathbf{H}_{rrr}^- + D_5\mathbf{H}_{rr}^- + E_5\mathbf{H}_r^- + F_5\mathbf{H}$$

where

$$\begin{aligned}C_3 &= \begin{pmatrix} 1 & 0 \\ 0 & n_2^2/n_1^2 \end{pmatrix}, \\ D_3 &= \begin{pmatrix} 0 & 0 \\ m(n_2^2/n_1^2 - 1)/r^* & 2(n_2^2/n_1^2 - 1)/r^* \end{pmatrix}, \\ C_5 &= \begin{pmatrix} 0 & 0 \\ 0 & -2(n_2^2/n_1^2 - 1)/r^* \end{pmatrix}, \\ D_5 &= \begin{pmatrix} -2k^2(n_2^2 - n_1^2) & 0 \\ -2m(n_2^2/n_1^2 - 1)/r^{*2} & -2k^2(n_2^2 - n_1^2) - 4(n_2^2/n_1^2 - 1)/r^{*2} \end{pmatrix}, \\ E_3 &= \begin{pmatrix} -k^2(n_2^2 - n_1^2) & -2m^2(n_2^2/n_1^2 - 1)/r^{*2} \\ -m(n_2^2/n_1^2 - 1)/r^{*2} & -k^2(n_2^2 - n_1^2)n_2^2/n_1^2 + 2(n_2^2/n_1^2 - 1)/r^{*2} \end{pmatrix}, \\ E_5 &= \begin{pmatrix} 0 & -12m(n_2^2/n_1^2 - 1)/r^{*3} \\ 2m(n_2^2/n_1^2 - 1)/r^{*3} & 2k^2(n_2^2/n_1^2 - 1)(n_2^2 - n_1^2)/r^* - (4m^2 + 10)(n_2^2/n_1^2 - 1)/r^{*3} \end{pmatrix}\end{aligned}$$

The elements of the other two matrices are

$$\begin{aligned}
[F_3]_{11} &= \frac{k^2}{r^*}(n_2^2 - n_1^2) + 2m^2 \frac{n_2^2/n_1^2 - 1}{r^{*3}} \\
[F_3]_{12} &= 2m^2 \frac{n_2^2/n_1^2 - 1}{r^{*3}} \\
[F_3]_{21} &= -m \frac{n_2^2/n_1^2 - 1}{r^*} k^2(n_2^2 - n_1^2) + 4m^2 \frac{n_2^2/n_1^2 - 1}{r^{*3}} \\
[F_3]_{22} &= -\frac{k^2}{r^*} \frac{n_2^2}{n_1^2} (n_2^2 - n_1^2) + 4 \frac{n_2^2/n_1^2 - 1}{r^{*3}} \\
[F_5]_{11} &= k^4(n_2^2 - n_1^2)^2 - \frac{3k^2}{r^{*2}}(n_2^2 - n_1^2) - 12m^2 \frac{n_2^2/n_1^2 - 1}{r^{*4}} \\
[F_5]_{12} &= -12m \frac{n_2^2/n_1^2 - 1}{r^{*4}} \\
[F_5]_{21} &= 2m \frac{n_2^2/n_1^2 - 1}{r^{*2}} k^2(n_2^2 - n_1^2)^2 - 2(2m^2 + 7)m \frac{n_2^2/n_1^2 - 1}{r^{*4}} \\
[F_5]_{22} &= k^4(n_2^2 - n_1^2)^2 + \frac{2n_2^2/n_1^2 - 5}{r^{*2}} k^2(n_2^2 - n_1^2) - (8m^2 + 14) \frac{n_2^2/n_1^2 - 1}{r^{*4}} + 4m^2 \frac{n_2^2/n_1^2 - 1}{r^{*4}}
\end{aligned}$$

Since higher derivative are present we must complete the system of equations by expanding the right hand side as follows

$$\begin{aligned}
\beta^2 \mathbf{H}_j &= \beta^2 \left(\mathbf{H} + (r_j - r^*) \mathbf{H}_r^- + \frac{1}{2} (r_j - r^*)^2 \mathbf{H}_{rr}^- \right) \\
&= \underbrace{\mathbf{H} + \frac{1}{r^*} \mathbf{H}_r^- + B_1 \mathbf{H}_{rr}^-}_{\beta^2 \mathbf{H}} + (r_j - r^*) \underbrace{\left(\mathbf{H}_{rrr}^- + \frac{1}{r^*} \mathbf{H}_{rr}^- + B_2 \mathbf{H}_r^- + B_3 \mathbf{H} \right)}_{\beta^2 \mathbf{H}_r^-} \\
&\quad + \underbrace{\frac{1}{2} (r_j - r^*)^2 \left(\mathbf{H}_{rrrr}^- + \frac{1}{r^*} \mathbf{H}_{rrr}^- + B_4 \mathbf{H}_{rr}^- + B_5 \mathbf{H}_r^- + B_6 \mathbf{H} \right)}_{\beta^2 \mathbf{H}_{rr}^-}
\end{aligned}$$

where we have differentiated Eq. (10) twice and used the appropriate continuity conditions. Also,

$$\begin{aligned}
B_2 &= \begin{pmatrix} k^2 n^2 - (m^2 + 2)/r^{*2} & -2m/r^{*2} \\ -2m/r^{*2} & k^2 n^2 - (m^2 + 2)/r^{*2} \end{pmatrix}, \\
B_3 &= \begin{pmatrix} 2(m^2 + 1)/r^{*3} & 4m/r^{*3} \\ 4m/r^{*3} & 2(m^2 + 1)/r^{*3} \end{pmatrix}, \\
B_4 &= \begin{pmatrix} k^2 n^2 - (m^2 + 3)/r^{*3} & -2m/r^{*3} \\ -2m/r^{*3} & k^2 n^2 - (m^2 + 3)/r^{*3} \end{pmatrix}, \\
B_5 &= \begin{pmatrix} (4m^2 + 6)/r^{*3} & 8m/r^{*3} \\ 8m/r^{*3} & (4m^2 + 6)/r^{*3} \end{pmatrix}, \\
B_6 &= \begin{pmatrix} -6(m^2 + 1)/r^{*4} & -12m/r^{*4} \\ -12m/r^{*4} & -6(m^2 + 1)/r^{*4} \end{pmatrix}
\end{aligned}$$

Now, we can form a system of algebraic equations to determine all the unknown coefficients. This is done as before, by equating the coefficients of \mathbf{H}_{rrrr}^- , \mathbf{H}_{rrr}^- , \mathbf{H}_{rr}^- , \mathbf{H}_r^- and \mathbf{H} at $r < r^*$ and their (+) counterparts at $r > r^*$. Thus at $r = r_j < r^*$

$$\begin{aligned}
\Gamma_1 + \Gamma_2 + \Gamma_3 + S_1(j+1)\Gamma_4 + S_1(j+2)\Gamma_5 &= B_1 + (r_j - r^*)B_3 + \frac{1}{2}(r_j - r^*)^2B_6 \\
(r_{j-2} - r^*)\Gamma_1 + (r_{j-1} - r^*)\Gamma_2 + (r_j - r^*)\Gamma_3 + S_2(j+1)\Gamma_4 + S_2(j+2)\Gamma_5 &= \\
&\quad \frac{1}{r^*}I_2 + (r_j - r^*)B_2 + \frac{1}{2}(r_j - r^*)^2B_5 \\
\frac{1}{2}(r_{j-2} - r^*)^2\Gamma_1 + \frac{1}{2}(r_{j-1} - r^*)^2\Gamma_2 + \frac{1}{2}(r_j - r^*)^2\Gamma_3 + S_3(j+1)\Gamma_4 + S_3(j+2)\Gamma_5 &= \\
&\quad I_2 + \frac{(r_j - r^*)}{r^*}I_2 + \frac{1}{2}(r_j - r^*)^2B_4 \\
\frac{1}{6}(r_{j-2} - r^*)^3\Gamma_1 + \frac{1}{6}(r_{j-1} - r^*)^3\Gamma_2 + \frac{1}{6}(r_j - r^*)^3\Gamma_3 + S_4(j+1)\Gamma_4 + S_4(j+2)\Gamma_5 &= \\
&\quad (r_j - r^*)I_2 + \frac{1}{2r^*}(r_j - r^*)^2I_2 \\
\frac{1}{24}(r_{j-2} - r^*)^4\Gamma_1 + \frac{1}{24}(r_{j-1} - r^*)^4\Gamma_2 + \frac{1}{24}(r_j - r^*)^4\Gamma_3 + S_5(j+1)\Gamma_4 + S_5(j+2)\Gamma_5 &= \\
&\quad \frac{1}{2}(r_j - r^*)^2I_2
\end{aligned}$$

where $S_1(j) = I_2 + (r_j - r^*)D_1 + \frac{1}{2}(r_j - r^*)^2F_1 + \frac{1}{6}(r_j - r^*)^3F_3 + \frac{1}{24}(r_j - r^*)^4F_4$, $S_2(j) = (r_j - r^*)C_1 + \frac{1}{2}(r_j - r^*)^2E_1 + \frac{1}{6}(r_j - r^*)^3E_3 + \frac{1}{24}(r_j - r^*)^4E_5$, $S_3(j) = \frac{1}{2}(r_j - r^*)^2I_2 + \frac{1}{6}(r_j - r^*)^3D_3 + \frac{1}{24}(r_j - r^*)^4D_5$, $S_4(j) = \frac{1}{6}(r_j - r^*)^3C_3 + \frac{1}{24}(r_j - r^*)^4C_5$ and $S_5(j) = \frac{1}{24}(r_j - r^*)^4I_2$. At $r = r_{j+1} > r^*$

$$\begin{aligned}
S_6(j-1)\Gamma_1 + S_6(j)\Gamma_2 + \Gamma_3 + \Gamma_4 + \Gamma_5 &= B_1 + (r_{j+1} - r^*)B_3 + \frac{1}{2}(r_{j+1} - r^*)^2B_6 \\
S_7(j-1)\Gamma_1 + S_7(j)\Gamma_2 + (r_{j+1} - r^*)\Gamma_3 + (r_{j+2} - r^*)\Gamma_4 + (r_{j+3} - r^*)\Gamma_5 &= \\
&\quad \frac{1}{r^*}I_2 + (r_{j+1} - r^*)B_2 + \frac{1}{2}(r_{j+1} - r^*)^2B_5 \\
S_8(j-1)\Gamma_1 + S_8(j)\Gamma_2 + \frac{1}{2}(r_{j+1} - r^*)^2\Gamma_3 + \frac{1}{2}(r_{j+2} - r^*)^2\Gamma_4 + \frac{1}{2}(r_{j+3} - r^*)^2\Gamma_5 &= \\
&\quad I_2 + \frac{(r_{j+1} - r^*)}{r^*}I_2 + \frac{1}{2}(r_{j+1} - r^*)^2B_4 \\
S_9(j-1)\Gamma_1 + S_9(j)\Gamma_2 + \frac{1}{6}(r_{j+1} - r^*)^3\Gamma_3 + \frac{1}{6}(r_{j+2} - r^*)^3\Gamma_4 + \frac{1}{6}(r_{j+3} - r^*)^3\Gamma_5 &= \\
&\quad (r_{j+1} - r^*)I_2 + \frac{1}{2r^*}(r_{j+1} - r^*)^2I_2 \\
S_{10}(j-1)\Gamma_1 + S_{10}(j)\Gamma_2 + \frac{1}{24}(r_{j+1} - r^*)^4\Gamma_3 + \frac{1}{24}(r_{j+2} - r^*)^4\Gamma_4 + \frac{1}{24}(r_{j+3} - r^*)^4\Gamma_5 &= \\
&\quad \frac{1}{2}(r_{j+1} - r^*)^2I_2
\end{aligned}$$

where $S_6(j) = I_2 + (r_j - r^*)D_2 + \frac{1}{2}(r_j - r^*)^2F_2 + \frac{1}{6}(r_j - r^*)^3F_4 + \frac{1}{24}(r_j - r^*)^4F_6$, $S_7(j) = (r_j - r^*)C_2 + \frac{1}{2}(r_j - r^*)^2E_2 + \frac{1}{6}(r_j - r^*)^3E_4 + \frac{1}{24}(r_j - r^*)^4E_6$, $S_8(j) = \frac{1}{2}(r_j - r^*)^2I_2 + \frac{1}{6}(r_j - r^*)^3D_4 + \frac{1}{24}(r_j - r^*)^4D_6$, $S_9(j) = \frac{1}{6}(r_j - r^*)^3C_4 + \frac{1}{24}(r_j - r^*)^4C_6$ and $S_{10}(j) = \frac{1}{24}(r_j - r^*)^4I_2$. The systems at the points $r = r_{j-1}$ and $r = r_{j-2}$ are obtained in a similar manner and will not be explicitly given here.

To demonstrate the convergence of the method we choose a fiber with multiple layers that can support both TE and TM modes. Consider a fiber consisting of an air core of radius $5\mu\text{m}$ and a series of alternating layers of radii $1\mu\text{m}$ and refractive indices $n_1 = 2$ and $n_2 = 1$, respectively. The results for the propagating constant for the TE and TM modes are shown in Table 1. In Fig. 5 the corresponding TE and TM modes are shown. The $m = 1$

Mode	Propagation constant					
	N=500	N=1000	N=2000	N=4000	N=10000	N=20000
TM	0.52520655	0.52731320	0.52714039	0.52707988	0.52706043	0.52705446
4th order	0.52732576	0.52707445	0.52705720	0.52705650	0.52705645	0.52705645
TE	0.78582132	0.78580424	0.78588272	0.78590279	0.78590848	0.78590929
4th order	0.78334621	0.78575156	0.78588122	0.78590670	0.78590941	0.78590954

Table 1: The propagation constants for the multi-layered fiber of the text.

case is again described in the appendix.

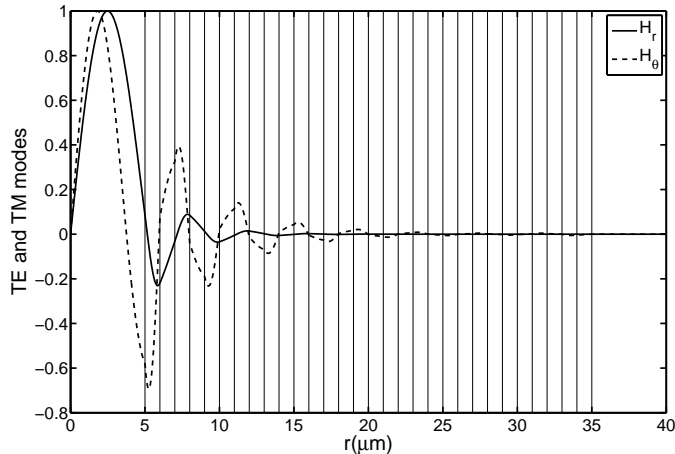


Figure 5: The TE and TM modes respectively corresponding to the propagation constants of Table 1.

One can go to even higher higher accuracy. In fact in Ref. [28] the authors have obtained sixteenth order accuracy. This, however, introduces a fundamental limitation, namely the number of irregular points. In order for the method to work, one must have a minimum number of points between interfaces. When the structure of the fiber become more complicated it is obvious that this is a serious limitation. We demonstrate how to overcome this in the following section.

5. Coordinate stretching transformation

One of the problems one might encounter in this formalism is the total number of points in a grid that must be used to have high accuracy results. The number of grid points is directly proportional to the size of the matrix to be diagonalized, thus more points means more computational time. When the width of the fiber's core is considerably (orders of magnitude) larger than the width of the layers, such as in the case of the fibers in Refs. [2, 3, 4, 5, 29], one needs to use a sufficiently small numerical step size to insure that there exist at least two points per layer. If the number of points per interface is less than two, the assumption used in the derivation of the method is not true, and the method fails. This is because the method assumes that there is only one interface for each set of three grid points. Because the reflecting layers are small, this means that a small step size must be used. If one uses a uniform mesh, this means that in the core region one is using a step size that is much smaller than necessary, i.e., computational effort is being made unnecessarily.

To avoid this problem, we introduce a coordinate stretching by using a new independent variable ρ such that

$$\rho = \begin{cases} r, & r < R^* \\ R^* + \sigma(r - R^*), & r \geq R^* \end{cases}$$

Here R^* is the location of an additional artificial layer placed arbitrarily inside the core of the fiber and σ is a stretching parameter such that $\sigma > 1$. This transformation increases the effective width between the layers relative to the core (by a factor of σ). We will use uniformly spaced points in terms of ρ , which is equivalent to using a smaller step size in the core and a larger step size in the layers when measured in terms of r . Under this transformation, Eqs. (7) become

$$\mathbf{H}_{\rho\rho} + \frac{1}{\rho} \mathbf{H}_\rho + B\mathbf{H} = \beta^2 \mathbf{H}, \quad \rho < R^* \quad (13a)$$

$$\sigma^2 \mathbf{H}_{\rho\rho} + \frac{\sigma^2}{\rho + (\sigma - 1)R^*} \mathbf{H}_\rho + B\mathbf{H} = \beta^2 \mathbf{H}, \quad \rho \geq R^* \quad (13b)$$

At the point $\rho = R^*$ we impose the additional artificial jump conditions

$$\mathbf{H}^+ = \mathbf{H}^-, \quad \mathbf{H}_r^+ = \mathbf{H}_r^-$$

so that, in terms of the new coordinate, both fields are continuous and their derivatives satisfy

$$\sigma \mathbf{H}_\rho^+ = \mathbf{H}_\rho^-$$

It follows then, from Eq. (7) and the above jump conditions that the second derivatives satisfy

$$\sigma^2 \mathbf{H}_{\rho\rho}^+ = \mathbf{H}_{\rho\rho}^-$$

where the $(-)$ and $(+)$ regions are on the left and right of the discontinuity, respectively. At the real layers, including the core, Eqs. (9) apply, with appropriate changes, namely

$$r = \frac{\rho - R^*}{\sigma} + R^*, \quad \frac{d}{dr} = \sigma \frac{d}{d\rho}$$

The finite difference approximation in matrix form at all points is again

$$\Gamma_1 \mathbf{H}_{i-1} + \Gamma_2 \mathbf{H}_i + \Gamma_3 \mathbf{H}_{i+1} = \beta^2 \mathbf{H}_i$$

where the Γ 's are 2×2 matrices. As always, we need to expand \mathbf{H}_{i-1} , \mathbf{H}_i and \mathbf{H}_{i+1} around the points of the grid that include the discontinuity. Assuming that $r_j \leq R^* < r_{j+1}$, the systems that determine the finite difference coefficients at these regions then satisfy the following systems

At $\rho_j \leq R^*$

$$\begin{aligned} \Gamma_1 + \Gamma_2 + \Gamma_3 &= B \\ (\rho_{j-1} - R^*)\Gamma_1 + (\rho_j - R^*)\Gamma_2 + \Gamma_3(\rho_{j+1} - R^*)/\sigma &= \frac{1}{R^*} I_2 \\ \frac{1}{2}(\rho_{j-1} - R^*)^2 \Gamma_1 + \frac{1}{2}(\rho_j - R^*)^2 \Gamma_2 + \frac{1}{2\sigma^2}(\rho_{j+1} - R^*)^2 \Gamma_3 &= I_2 \end{aligned}$$

At $\rho_{j+1} > R^*$

$$\begin{aligned} \Gamma_1 + \Gamma_2 + \Gamma_3 &= B \\ \sigma(\rho_j - R^*)\Gamma_1 + (\rho_{j+1} - R^*)\Gamma_2 + \Gamma_3(\rho_{j+2} - R^*) &= \frac{\sigma}{R^*} I_2 \\ \frac{\sigma^2}{2}(\rho_j - R^*)^2 \Gamma_1 + \frac{1}{2}(\rho_{j+1} - R^*)^2 \Gamma_2 + \frac{1}{2}(\rho_{j+2} - R^*)^2 \Gamma_3 &= \sigma^2 I_2 \end{aligned}$$

The finite difference coefficients for the rest points are determined as usual to be, at $\rho_j \leq \rho^*$

$$\begin{aligned} \Gamma_1 + \Gamma_2 + \Gamma_3 \left[I_2 + (\rho_{j+1} - \rho^*)D + \frac{1}{2}(\rho_{j+1} - \rho^*)^2 F \right] &= B^- \\ (\rho_{j-1} - \rho^*)\Gamma_1 + (\rho_j - \rho^*)\Gamma_2 + \Gamma_3 \left[(\rho_{j+1} - \rho^*)C + \frac{1}{2}(\rho_{j+1} - \rho^*)^2 E \right] &= \frac{\sigma}{\rho^*} I_2 \\ \frac{1}{2}(\rho_{j-1} - \rho^*)^2 \Gamma_1 + \frac{1}{2}(\rho_j - \rho^*)^2 \Gamma_2 + \frac{1}{2}(\rho_{j+1} - \rho^*)^2 \Gamma_3 &= \sigma^2 I_2 \end{aligned}$$

and $\rho_j > \rho^*$

$$\begin{aligned} \Gamma_1 \left[I_2 - (\rho_j - \rho^*)C^{-1}D + \frac{1}{2}(\rho_j - \rho^*)^2 F_2 \right] + \Gamma_2 + \Gamma_3 &= B^+ \\ \Gamma_1 \left[(\rho_j - \rho^*)C^{-1} + \frac{1}{2}(\rho_j - \rho^*)^2 E_2 \right] + (\rho_{j+1} - \rho^*)\Gamma_2 + \Gamma_3(\rho_{j+2} - \rho^*) &= \frac{\sigma}{\rho^*} I_2 \\ \frac{1}{2}(\rho_j - \rho^*)^2 \Gamma_1 + \frac{1}{2}(\rho_{j+1} - \rho^*)^2 \Gamma_2 + \frac{1}{2}(\rho_{j+2} - \rho^*)^2 \Gamma_3 &= \sigma^2 I_2 \end{aligned}$$

where the matrices E and F are defined in section 2 and we need to introduce the matrices

$$E_2 = \begin{pmatrix} 0 & 0 \\ 0 & (1 - n_1^2/n_2^2)/\rho^* \end{pmatrix}, \quad F_2 = \begin{pmatrix} k^2(n_2^2 - n_1^2) & 0 \\ m(1 - n_1^2/n_2^2)/\rho^* & k^2(n_2^2 - n_1^2) - (1 - n_1^2/n_2^2)/\rho^{*2} \end{pmatrix}$$

Using the coordinate stretching more demanding structures can be analyzed using the same number of points. Consider, for example, the fiber described in Refs. [29, 30]. This fiber consists of a hollow-core $316\text{ }\mu\text{m}$ in radius surrounded by 70 alternating layers of As_2Se_3 $0.27\text{ }\mu\text{m}$ thick, and polyether imide $0.47\text{ }\mu\text{m}$ thick. The fundamental photonic bandgap is centered at $\lambda = 2.28\text{ }\mu\text{m}$ and the refractive indices of the layers are $n_1 = 2.8$ and $n_2 = 1.55 + 1.0 \times 10^{-4} i$, respectively. The effective indices are found to be $0.99999032 + 1.4 \times 10^{-12} i$ and $0.99999025 + 7.1 \times 10^{-11} i$ for the TE and TM modes, respectively. These results were obtained for 20000 points. Now consider the coordinate stretching transformation:

$$\rho = \begin{cases} r, & r < 300\mu\text{m} \\ 300\mu\text{m} + 5(r - 300\mu\text{m}), & r \geq 300\mu\text{m} \end{cases}$$

For 5000 points the IIM in its original formulation fails since the three points per interface fails. However, we can get results of good accuracy using the above transformation. Indeed, for 5000 points the results are for the effective index $0.99999030 + 1.39 \times 10^{-12} i$ and $0.99999021 + 6.9 \times 10^{-11} i$ for the TE and TM modes, respectively. In Fig. 6 one can see and compare the TE modes obtained with and without the coordinate stretching. It is apparent that part from the added interface the fields are identical. This transformation proves very useful for demanding structures such as this one.

6. Conclusions

We presented a numerical method based on the immersed interface method that can be used to obtain the propagation modes of circularly symmetric Bragg fibers with arbitrary index profiles. In its original formulation the method is second order accurate and was applied to boundary value problems with discontinuous and/or singular coefficients. We extended this method to matrix eigenvalue problems and to higher accuracy. Cumbersome integrations or finding roots of nontrivial functions, such as Bessel functions, are avoided and computational time is minimized without sacrificing accuracy. All modes can be determined and excellent results are achieved even for fibers with complicated structure. Even when the geometry of the fiber is rather demanding, as in Omniduide fibers, a coordinate stretching can be applied to keep computation time to a minimum.

Acknowledgements

I am very grateful to W.L. Kath for his help and support concerning this work.

Appendix A. Finite difference approximations for first and second derivatives

For the second order scheme

$$\begin{aligned} \frac{dH}{dr} &= \frac{H_{i+1} - H_{i-1}}{2h} \\ \frac{d^2H}{dr^2} &= \frac{H_{i+1} - 2H_i + H_{i-1}}{h^2} \end{aligned}$$

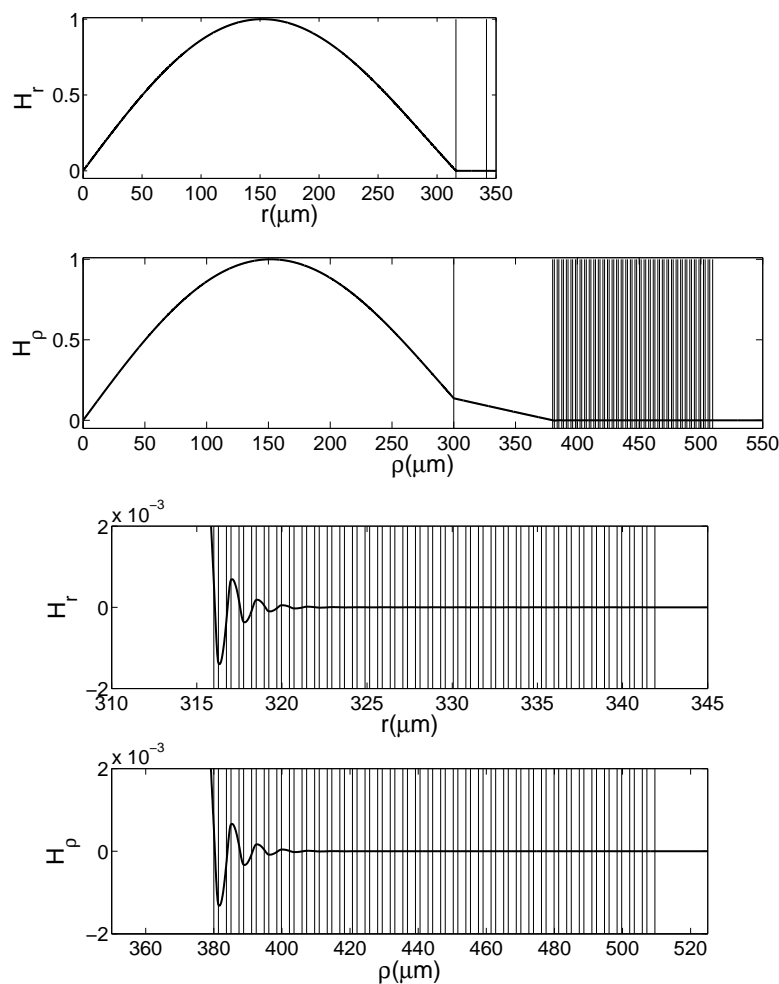


Figure 6: The TE mode of an Omniguide fiber using the original IIM and the coordinate stretching transformation. In the first figure only the first and last layers are plotted.

and for the fourth order case

$$\begin{aligned}\frac{dH}{dr} &= \frac{-H_{i+2} + 8H_{i+1} - 8H_{i-1} + H_{i-2}}{12h} \\ \frac{d^2H}{dr^2} &= \frac{-H_{i+2} + 16H_{i+1} - 30H_i + 16H_{i-1} - H_{i-2}}{12h^2}\end{aligned}$$

Appendix B. Boundary conditions for higher-order differences

As usual, special care must be given to the end points. High-order methods require an extrapolation scheme to determine the differencing coefficients at r_2 and r_{N-1} . Given the boundary conditions $\mathbf{H}(r_1) = \mathbf{H}_1 = 0$ and $\mathbf{H}(r_N) = \mathbf{H}_N = 0$ we use the extrapolation

$$\begin{aligned}\mathbf{H}_2 &= -\mathbf{H}_6 + 4\mathbf{H}_5 - 6\mathbf{H}_4 + 4\mathbf{H}_3 \\ \mathbf{H}_{N-1} &= 4\mathbf{H}_{N-2} - 6\mathbf{H}_{N-3} + 4\mathbf{H}_{N-4} - \mathbf{H}_{N-5}\end{aligned}$$

to accommodate for these extra points.

Appendix C. Special case boundary conditions ($m = 1$)

All of the cases considered had the fields tend to zero at the boundaries, namely at $r = 0$ and $r \rightarrow \infty$. However, this is not the case for the calculation of the HE_{11} mode (our $m = 1$ case). Indeed, recall that the boundary conditions for this case are

$$H_r + H_\theta = 0 \quad \text{and} \quad \frac{d}{dr}(H_r - H_\theta) = 0$$

at $r = 0$. To accommodate this we need to alter the finite difference scheme to include the new boundary conditions.

Appendix C.1. The second order correction

At the first point where $i = 1$ Eqs. (6) become

$$\gamma_1 H_{r,0} + \gamma_2 H_{r,1} + \gamma_3 H_{r,2} + \Delta H_{\theta,1} = \beta^2 H_{r,1} \quad (\text{C.1a})$$

$$\delta_1 H_{\theta,0} + \delta_2 H_{\theta,1} + \delta_3 H_{\theta,2} + \Gamma H_{r,1} = \beta^2 H_{\theta,1} \quad (\text{C.1b})$$

and the boundary conditions become under a second order approximation of the first derivative

$$H_{r,1} + H_{\theta,1} = 0 \quad \text{and} \quad H_{r,2} - H_{r,0} = H_{\theta,2} - H_{\theta,0}$$

Note that all the coefficients are known (we are not at an interface) and we only need to eliminate the two $H_{r,0}$ and $H_{\theta,0}$ terms.

Adding Eqs. (C.1) and taking the limit as $r \rightarrow 0$ gives (recall $\gamma_1 = \delta_1$, $\gamma_2 = \delta_2$, $\gamma_3 = \delta_3$ and $\Gamma = \Delta$ as clearly seen from their definition below Eqs. (6))

$$H_{r,2} + H_{r,0} = H_{\theta,2} + H_{\theta,0}$$

which suggests that

$$\mathbf{H}_0 = \mathbf{H}_2$$

Appendix C.2. The fourth order correction

At the first point where $i = 1$ we write the system as

$$\gamma_1 H_{r,-1} + \gamma_2 H_{r,0} + \gamma_3 H_{r,1} + \gamma_4 H_{r,2} + \gamma_5 H_{r,3} + \Delta H_{\theta,1} = \beta^2 H_{r,1} \quad (\text{C.2a})$$

$$\delta_1 H_{\theta,-1} + \delta_2 H_{\theta,0} + \delta_3 H_{\theta,1} + \delta_4 H_{\theta,2} + \delta_5 H_{\theta,3} + \Gamma H_{r,1} = \beta^2 H_{\theta,1} \quad (\text{C.2b})$$

where the definitions for the coefficients follow from Eq. (12). The steps here follow the procedure for the second order results. Thus, from the definition of the first derivative at fourth order for $i = 1$ we get

$$H_{r,-1} - 8H_{r,0} + 8H_{r,2} - H_{r,3} = H_{\theta,-1} - 8H_{\theta,0} + 8H_{\theta,2} - H_{\theta,3}$$

As above adding Eqs. (C.2) and taking the limit $r \rightarrow 0$ gives

$$\frac{1}{12}(H_{r,-1} + H_{\theta,-1}) - \frac{2}{3}(H_{r,0} + H_{\theta,0}) + \frac{2}{3}(H_{r,2} + H_{\theta,2}) - \frac{1}{12}(H_{r,3} + H_{\theta,3}) = 0 \quad (\text{C.3})$$

However, we also need to extrapolate for the point $i = -1$, namely

$$\mathbf{H}_{-1} = 4\mathbf{H}_0 - 6\mathbf{H}_1 + 4\mathbf{H}_2 - \mathbf{H}_3 \quad (\text{C.4})$$

Note that while the point $i = 0$ was before ignored this is not the case here. Using these equations we can now eliminate the point $i = 0$ as follows

$$\mathbf{H}_0 = -\frac{3}{2}\mathbf{H}_1 + 3\mathbf{H}_2 - \frac{1}{2}\mathbf{H}_3$$

References

References

- [1] P. Yeh, A. Yariv, E. Marom, Theory of Bragg fiber, *J. Opt. Soc. Am.* 68 (1978) 1196–1201.
- [2] Y. Fink, J. N. Winn, F. Shanhui, J. M. C. Chiping, J. D. Joannopoulos, E. L. Thomas, A dielectric omnidirectional reflector, *Science* 282 (1998) 1679–1682.
- [3] B. Temelkuran, S. D. Hart, G. Benolt, J. D. Joannopoulos, Y. Fink, Wavelength-scalable hollow optical fibres with large photonic bandgaps for CO₂ laser transmission, *Nature* 420 (2002) 650–653.
- [4] M. Ibanescu, Y. Fink, S. Fan, E. L. Thomas, J. D. Joannopoulos, An all-dielectric coaxial waveguide, *Science* 289 (2000) 415–419.
- [5] S. G. Johnson, M. Ibanescu, M. Skorobogatiy, O. Weisberg, T. D. Engeness, M. Soljacic, S. A. Jacobs, J. D. Joannopoulos, Y. Fink, Analysis of mode structure in hollow dielectric waveguide fibers, *Opt. Express* 9 (2001) 748–779.
- [6] Y. Xu, R. K. Lee, A. Yariv, Asymptotic analysis of Bragg fibers, *Opt. Lett.* 25 (2000) 1756–1758.
- [7] S. Guo, S. Albin, Comparative analysis of Bragg fibers, *Opt. Express* 12 (2004) 198–207.
- [8] M. Eguchi, S. Horinouchi, All propagation modes of large-core multimode optical fibers with an arbitrary core profile, *Opt. Lett.* 29 (2004) 1051–1053.
- [9] M. Eguchi, Finite-element modal analysis of multistep-index large-core multimode fibers, *J. Opt. Soc. Am. B* 27 (2010) 1464–1474.
- [10] T. Kawanishi, M. Izutsu, Coaxial periodic optical waveguide, *Opt. Express* 7 (2000) 10–22.

- [11] J. Sakai, P. Nouchi, Propagation properties of Bragg fiber analyzed by a Hankel function formalism, *Opt. Comm.* 249 (2005) 153163.
- [12] S. Guo, F. Wu, K. Ikram, S. Albin, Analysis of circular fibers with an arbitrary index profile by the Galerkin method, *Opt. Lett.* 29 (2004) 32–34.
- [13] S. Barai, A. Sharma, Wavelet-Galerkin solver for the analysis of optical waveguides, *J. Opt. Soc. Am. A* 26 (2009) 931–937.
- [14] Z. Li, An overview of the immersed interface method and its applications, *Taiwanese Journal of Mathematics* 7 (2003) 1–49.
- [15] R. J. Leveque, Z. Li, The immersed interface method for elliptic equations with discontinuous coefficients and singular sources, *SIAM J. Numer. Anal.* 31 (1994) 1019–1044.
- [16] X. Zhong, A new high-order immersed interface method for solving elliptic equations with imbedded interface of discontinuity, *J. Comput. Phys.* 225 (2007) 1066–1099.
- [17] P. A. Berthelsen, A decomposed immersed interface method for variable coefficient elliptic equations with non-smooth and discontinuous solutions, *J. Comput. Phys.* 197 (2004) 364386.
- [18] S. Xu, Z. J. Wang, An immersed interface method for simulating the interaction of a fluid with moving boundaries, *J. Comput. Phys.* 216 (2006) 454–493.
- [19] D. V. Le, B. C. Khoo, J. Peraire, An immersed interface method for viscous incompressible flows involving rigid and flexible boundaries, *J. Comput. Phys.* 220 (2006) 109138.
- [20] K. Karagiozis, R. Kamakoti, C. Pantano, A low numerical dissipation immersed interface method for the compressible Navier-Stokes equations, *J. Comput. Phys.* 229 (2010) 701727.
- [21] T. P. Horikis, Eigenstate calculation of arbitrary quantum structures, *Phys. Lett. A* 359 (2006) 345348.
- [22] D. J. Costinett, T. P. Horikis, High-order eigenstate calculation of arbitrary quantum structures, *J. Phys. A: Math. Theor.* 42 (2009) 235201.
- [23] S. Deng, On the immersed interface method for solving time-domain Maxwell's equations in materials with curved dielectric interfaces, *Comput. Phys. Commun.* 179 (2008) 791800.
- [24] V. Rutka, Z. Li, An explicit jump immersed interface method for two-phase Navier-Stokes equations with interfaces, *Comput. Methods Appl. Mech. Engrg.* 197 (2008) 23172328.
- [25] W. Snyder, J. D. Love, Optical waveguide theory, Chapman & Hall, 1983.
- [26] J. Scheuer, A. Yariv, Annular Bragg defect mode resonators, *J. Opt. Soc. Am. B* 20 (2003) 2285–2291.
- [27] M. Skorobogatiy, K. Saitoh, M. Koshiba, Resonant directional coupling of hollow Bragg fibers, *Opt. Lett.* 29 (2004) 2112–2114.
- [28] Y. C. Zhou, S. Zhao, M. Feig, G. W. Wei, High order matched interface and boundary method for elliptic equations with discontinuous coefficients and singular sources, *J. Comput. Phys.* 213 (2006) 1–30.
- [29] K. Kuriki, O. Shapira, S. D. Hart, G. Benoit, Y. Kuriki, J. F. Viens, M. Bayindir, J. D. Joannopoulos and Y. Fink, Hollow multilayer photonic bandgap fibers for NIR applications, *Opt. Express* 12 (2004) 1510–1516.
- [30] T. P. Horikis, W. L. Kath, Modal analysis of circular Bragg fibers with arbitrary index profiles, *Opt. Lett.* 31 (2006) 3417–3419.